ILETA International Information and Engineering Technology Association

International Journal of Heat and Technology

Vol. 43, No. 5, October, 2025, pp. 1855-1861

Journal homepage: http://iieta.org/journals/ijht

Performance Optimization of Hybrid MWCNT-CuO Nanofluids in Sinusoidal Corrugated Plate Heat Exchangers



K.N.V. Sreedevi^{1*}, Naga Sarada Somanchi²

- ¹ Department of Mechanical Engineering, Chaitanya Bharathi Institute of Technology (A), Hyderabad 500075, India
- ² Mechanical Engineering Department, JNTUHUCESTH, Hyderabad 500085, India

Corresponding Author Email: knvsreedevi mech@cbit.ac.in

Copyright: ©2025 The authors. This article is published by IIETA and is licensed under the CC BY 4.0 license (http://creativecommons.org/licenses/by/4.0/).

https://doi.org/10.18280/ijht.430524

Received: 31 July 2025 Revised: 29 September 2025 Accepted: 11 October 2025 Available online: 31 October 2025

Keywords:

corrugated plate, wavy, pumping power, nanoparticle, optimum, flow rate, turbulence

ABSTRACT

Research on nanofluids has predominantly focused on single-component suspensions, while the potential of hybrid nanofluids-engineered by dispersing dissimilar nanoparticles within a base fluid-remains underexplored. Hybrid nanofluids offer the possibility of tailoring thermophysical properties by leveraging the complementary advantages of individual nanoparticles, such as the high aspect ratio and enhanced thermal percolation pathways of multi-walled carbon nanotubes (MWCNTs) and the favourable thermal conductivity of copper oxide (CuO). In this study, the convective heat transfer performance and hydrodynamic characteristics of hybrid MWCNT-CuO nanofluids in water were systematically investigated within both flat plate and sinusoidal corrugated plate heat exchangers (CPHEs). Mass ratios of MWCNT:CuO (1:1, 1:2, 2:1, 3:1, and 1:3) were prepared, and the effects of corrugation angle (30°, 40°, 50°, and 60°) and flow rate were examined. Key performance indicators including the convective heat transfer coefficient, heat transfer rate, and pressure drop were measured and subsequently optimised using Design-Expert software. Results demonstrated that corrugation mitigated fouling and scaling while enhancing turbulence, thereby significantly improving thermal performance compared with flat plates. The optimal hybrid composition achieved a favourable trade-off between heat transfer enhancement and pumping power penalties, highlighting the synergistic interactions between MWCNTs and CuO nanoparticles. Furthermore, the study revealed that the thermohydraulic performance factor is strongly dependent on both nanoparticle mass ratio and corrugation angle, with tailored properties achievable through careful parameter selection. These findings establish hybrid nanofluids as a versatile platform for application-specific thermal management solutions and provide novel insights into the optimisation of CPHEs.

1. INTRODUCTION

Techniques for enhancing heat transfer are of critical importance across a wide range of industrial sectors, including food processing, chemical production, power generation, and automotive thermal management. Heat exchangers serve as essential devices in these applications, facilitating the exchange of thermal energy between two or more fluids. The principal design requirements for modern heat exchangers include cost-effectiveness, compactness, and energy efficiency. Depending on the application, heat exchangers may be classified into direct-contact and indirect-contact configurations, with compact designs receiving growing attention due to increasing demands for enhanced thermal performance.

CPHEs have emerged as highly efficient systems owing to their distinctive surface geometries. In particular, sinusoidal wavy CPHEs promote turbulence and secondary flow even at relatively low Reynolds numbers, thereby augmenting convective heat transfer and reducing the likelihood of fouling and scaling [1, 2]. In such geometries, fluid streams undergo

repeated splitting and recombination, which improves mixing and thermal boundary layer disruption [3-5]. These advantages have stimulated significant research into CPHEs as candidates for high-performance thermal management systems.

Parallel to geometric enhancement strategies, nanofluids have been developed to exploit the extraordinary thermal properties of nanomaterials. Nanofluids, defined as suspensions of nanoparticles within a base fluid, provide tunable thermophysical properties that can surpass those of conventional working fluids [6-12]. Recent research has expanded into hybrid nanofluids, in which dissimilar nanoparticles are co-dispersed to create synergistic effects. For instance, Sunden et al. [13] demonstrated that the effective thermal conductivity of Al₂O₃-MWCNT/water nanofluids exceeded that of single-component nanofluids, while Han et al. [14] observed enhanced conductivity in hybrid suspensions of carbon nanotubes linked with iron and alumina oxide nanoparticles. Similarly, Suresh et al. [15] reported improved Nusselt numbers for Cu-Al₂O₃/water nanofluids at Reynolds numbers around 1730. Labib et al. [16] experimentally confirmed significant improvements in thermal characteristics when using CNT–Al₂O₃/water hybrid nanofluids, whereas Pandey et al. [17] observed consistent enhancements across all tested particle loadings for Al₂O₃/water suspensions.

Further comprehensive reviews have highlighted both the promise and the research gaps of hybrid nanofluids. Sarkar et al. [18] summarized developments on hybrid nanofluids such as MWNT-HEG/water, graphene-MWNT/water, Fe₂O₃-MWNT/water, SiO₂/MWCNT, and Ag-MWCNT/water, but reported a paucity of systematic studies on MWCNT-CuO/water systems. Likewise, Rafid et al. [19] underscored the scarcity of data regarding the thermophysical and hydrodynamic behaviour of MWCNT-CuO hybrid nanofluids, emphasizing the urgent need to investigate parameters such as thermal conductivity enhancement, optimal particle concentration, influence of flow rate, and overall system optimization.

Balashowry et al. [20] observed enhancement of thermal-conductivity, Coefficient-of-Performance with copper and alumina nanofluids in a condenser. Yahya et al. [21] found improvement in bending, bond and compressive strength with the use of ZrO₂-CNT in a sample. Nashee [22] concluded that cross-section has influence on heat transfer using water based Titanium Oxide Nanofluids.

Most existing studies have been directed towards relatively simple heat exchanger geometries and single-component nanofluids. Limited attention has been devoted to hybrid nanofluids operating in complex geometries such as corrugated channels, where coupled effects of particle composition, flow regime, and corrugation angle may yield distinct thermohydraulic responses. Furthermore, although both MWCNTs, as one-dimensional nanoparticles with exceptionally high aspect ratios, and CuO nanoparticles, as zero-dimensional oxides with inherently high thermal conductivity, are individually recognized for their potential in enhancing heat transfer, their combined effects in hybrid suspensions remain insufficiently characterized.

In this context, the performance of hybrid MWCNT–CuO/water nanofluids in sinusoidal CPHEs warrants systematic investigation. Particular attention is required to quantify the convective heat transfer coefficient, heat transfer rate, and associated pressure drop under varying nanoparticle ratios, flow rates, and corrugation angles. Addressing this knowledge gap is crucial for determining the optimum operating conditions and for developing predictive models capable of guiding the design of high-efficiency, application-specific heat exchangers.

2. METHODOLOGY

Schematic of plate angle and corrugated plate are represented in Figure 1 and Figure 2, respectively. The experimental setup consists of storage tanks and corrugated plates connected to pumps for both hot and cold fluids. Two rotameters were employed to measure the flow rates of the fluids, while a precision manometer was used to evaluate the pressure drop. Experiments were performed using both flat and wavy CPHEs with corrugation angles of 30°, 40°, and 50°. The detailed specifications of the CPHE are provided in Table 1.

Hot water (H₂O) was used as the heating fluid and maintained at a temperature of 70-74°C, while the hybrid nanofluid served as the cooling medium. The hot water was circulated through the lower channel of the CPHE with a

channel height of 1.5 cm, whereas the cold fluid was directed through the upper channel of 0.5 cm. A counter-current flow configuration was employed, with the cold fluid flow rate varied at 2, 3, and 4 L min⁻¹, while the hot water flow rate was maintained constant at 3 lpm.

Table 1. CPHE specifications

SLNO	Specification of Each Plate	Dimension
1.	length	30 cm
2.	width	10 cm
3.	angles	0, 30, 40, 50 degrees

Temperature measurements were carried out using thermocouples. Four thermocouples (T_1, T_{11}, T_2, T_3) were positioned at the inlet and outlet of the hot and cold streams, while seven thermocouples were attached to the middle plate separating the channels, enabling accurate wall temperature monitoring. All thermocouples were connected to a digital temperature indicator with an accuracy of $\pm 0.1\,^{\circ}\text{C}$. Readings were recorded after the system reached steady-state conditions.

The heat transfer rate was evaluated using Eqs. (1)-(3), while Eq. (4) was used to calculate the average wall temperature. The logarithmic mean temperature difference (LMTD) was determined from Eq. (5). The convective heat transfer coefficient, denoted by h, was obtained using Eq. (6). Pressure drop across the CPHE was calculated based on the difference in mercury levels in the U-tube manometer, as given in Eq. (7).

Experiments were performed with MWCNT–CuO/water hybrid nanofluids at an overall volume concentration of 0.09%. The hybrid nanofluid was prepared by combining MWCNT and CuO nanoparticles in different mass ratios: 1:1, 1:2, 2:1, 3:1, and 1:3. The influence of nanoparticle mass ratio on the heat transfer rate and pressure drop was systematically investigated.



Figure 1. Schematic of plate angle Θ



Figure 2. Schematic of corrugated plate

The thermophysical properties of the constituent nanoparticles were considered in the analysis. For MWCNTs,

the density, thermal conductivity, and specific heat capacity were 40 kg m⁻³, 2000 W m⁻¹ K⁻¹, and 733 J kg⁻¹ K⁻¹, respectively. For CuO, the density, thermal conductivity, and specific heat capacity were 6400 kg m⁻³, 32.9 W m⁻¹ K⁻¹, and 540 J kg⁻¹ K⁻¹, respectively. The overall nanoparticle volume fraction (Φ) was maintained at 0.09%. Based on the chosen mass ratio, the partial volume fractions of MWCNT (Φ 1) and CuO (Φ 2) were calculated accordingly. Table 2 presents the corresponding nanoparticle masses for each ratio.

$$Q_c = m_c C_c dt_c \tag{1}$$

$$Q_h = m_h C_h dt_h \tag{2}$$

$$Q_{avg} = \frac{Q_h + Q_c}{2} \tag{3}$$

$$Tavg = \frac{T4+T5+T6+T7+T8+T9+T10}{7}$$
 (4)

$$LMTD = ((T_avg - T_(c,in)) - (T_avg - T_(c,out)))/(ln (T_avg - T_(c,in))/(T_avg - T_(c,out)))$$
(5)

$$Qavg = h.A.LMTD (6)$$

$$Pressure drop = \Delta h \rho_{hyb} g \tag{7}$$

Table 2. Mass of nanoparticles

Nanoparticle Ratio	MWCNT gms per Litre	CuO gms per Litre
1:1	2.148	2.148
1:2	2.135	4.270
2:1	2.145	1.077
1:3	2.122	6.366
3:1	2.158	0.719

Thermophysical properties, viscosity, thermal conductivity, density, specific heat capacity of nanofluids, are calculated at bulk temperature using Eqs. (8)-(11) respectively.

$$\mu_{nf} = (1 + 2.5)\emptyset \mu_w \tag{8}$$

$$K_{nf} = \frac{k_{p+2k_w+2}\phi(k_p-k_w)(1+2.5\phi)}{k_p + 2k_w - \phi(k_p - k_w)} K_w$$
 (9)

$$\rho_{nf} = \emptyset \rho_n + (1 - \emptyset) \rho_w \tag{10}$$

$$C_{nf} = \frac{\left[\emptyset(\rho_{np}c_{np}) + (1-\emptyset)(\rho c_w)\right]}{\rho_{nf}} \tag{11}$$

Eqs. (12)-(14) represent formulas for hybrid nanofluids.

$$\rho_{hyb} = \emptyset_1 \rho_1 + \emptyset_2 \rho_2 + (1 - \emptyset_1 - \emptyset_2) \rho_w \tag{12}$$

$$C_{hyb} = \frac{\emptyset_1 \rho_1 \, c_1 + \emptyset_2 \rho_2 c_2 + (1 - \emptyset_1 - \emptyset_2) \rho_w c_w}{\rho_{hyb}} \tag{13}$$

$$k_{hyb} = \frac{k_1 + 2k_w + 2\emptyset_1(k_1 - k_w)}{k_1 + 2k_w - \emptyset_1(k_1 - k_w)} * \frac{k_2 + 2k_w + 2\emptyset_2(k_2 - k_w)}{k_2 + 2k_w - \emptyset_2(k_2 - k_w)} K_w$$
(14)

where, Φ_1 , ρ_1 , k_1 , c_1 are % volume concentration, density, thermal conductivity and specific heat of MWCNT/water and Φ_2 , ρ_2 , k_2 , c_2 are % volume concentration, density, thermal conductivity and specific heat of CuO/water in hybrid nanofluid.

3. RESULTS AND DISCUSSION

Figure 3 shows the influence of corrugated plate angle and nanoparticle ratio on the convective heat transfer coefficient (h). At a flow rate of 2 lpm, h attained a peak value of 1602 W/m²K at a corrugation angle of 60° with a 2:1 MWCNT:CuO nanoparticle ratio.

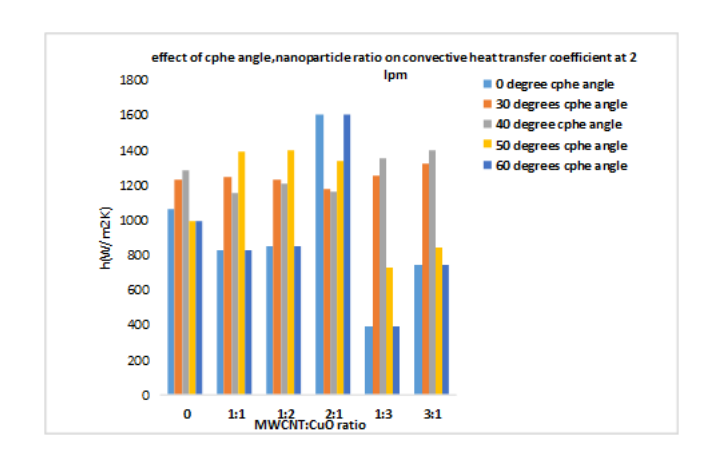


Figure 3. Effect of angle, nanoparticle ratio on h at 2 lpm

Figure 4 informs the details of relationship of plate angle, nanoparticle ratio on $h(W/m^2K)$ at 3 lpm, with a maximum of 2268.425 W/m^2K , at 30° and 1:2 ratio.

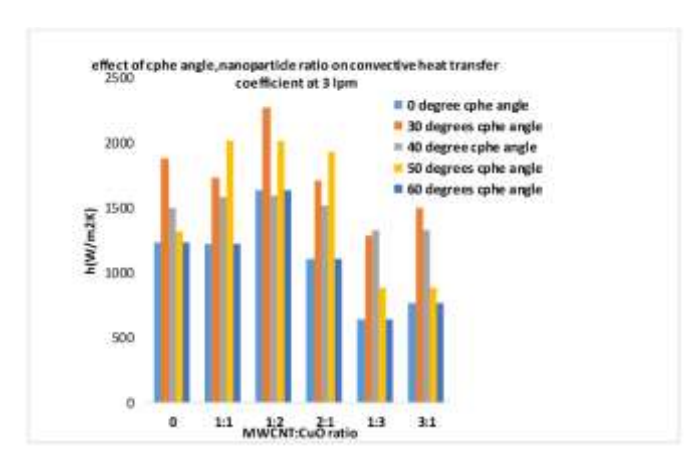


Figure 4. Effect of angle, nanoparticle ratio on h at 31 pm

An increase in the convective heat transfer coefficient (h) was observed with increasing flow rate and at a CPHE corrugation angle of 30°, attributed to enhanced turbulence, thinner thermal boundary layers, and improved fluid mixing. The 1:2 MWCNT:CuO mixture exhibited the best performance at higher flow rates (3 and 4 lpm), due to a favourable balance between the high thermal conductivity of MWCNTs and the stability of CuO. The 2:1 ratio was also effective at lower flow rates (2 lpm). In contrast, the 3:1 and 1:3 ratios resulted in reduced performance, likely due to increased viscosity or nanoparticle agglomeration.

Figure 5 illustrates the influence of these parameters on pressure drop. At a flow rate of 2 lpm, the minimum pressure drop of 7.3 Pa was observed for the flat plate CPHE with a 1:3 MWCNT:CuO ratio.

Figure 6 relates the influence of angle, nanoparticle ratio on h, at 4 lpm. Highest $h(W/m^2K)$ is $3021.942~W/m^2K$ at 30° , with a 1:2 particle ratio.

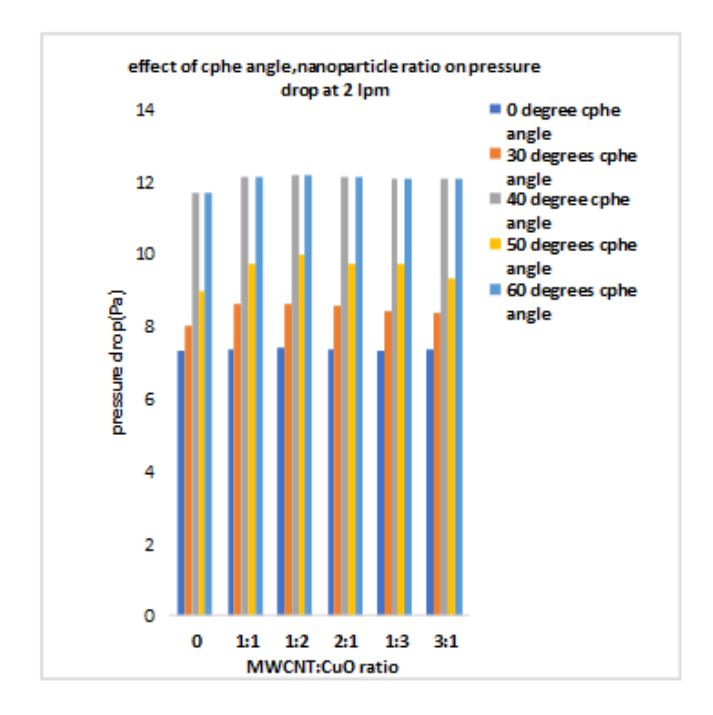


Figure 5. Effect of angle, nanoparticle ratio on pressure drop at 2 lpm

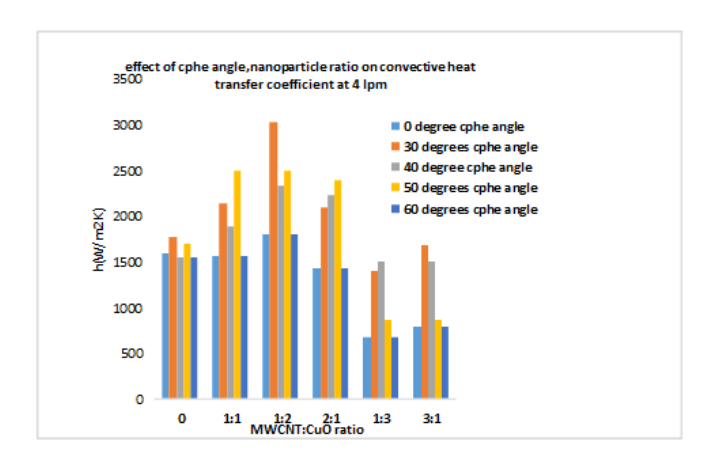


Figure 6. Effect of angle, nanoparticle ratio on h at 4 lpm

Figure 7 evaluates the impact of the parameters on pressure drop at 3 lpm. Optimized value of 6.90 Pascal was obtained for flat plates at a 1:3 nanoparticle ratio.

Figure 8 explains the influence of variables on pressure drop at 4lpm. Minimum pressure drop of 7.56Pa was found for flat plates at a 3:1 ratio of nano particles (MWCNT/CuO).

A reduction in pressure drop was observed when the flow rate increased from 2 to 3 lpm, attributed to reduced nanoparticle clustering and lower viscous effects. The primary factor influencing pressure drop was found to be the flow rate, with smaller corrugation angles, particularly the flat plate, exhibiting the lowest pressure drop. The introduction of nanoparticles generally elevated the pressure drop; however, variations in the MWCNT:CuO ratio had minimal impact

beyond a certain threshold.

Figures 9-11 illustrate the effects of CPHE corrugation angle and nanoparticle ratio on the average heat transfer rate $(Q_{av}g)$ at flow rates of 2, 3, and 4 lpm, respectively. The heat transfer rate increased with flow rate for all angles, primarily due to enhanced turbulence and Brownian motion of the hybrid nanofluids. While the convective heat transfer coefficient (h) represents the thermal transfer between the middle solid plate and the cold or test fluid, Q depends on the product of mass flow rate and specific heat capacity of the fluids $(m_h C_h, mcCc)$ and the temperature difference.

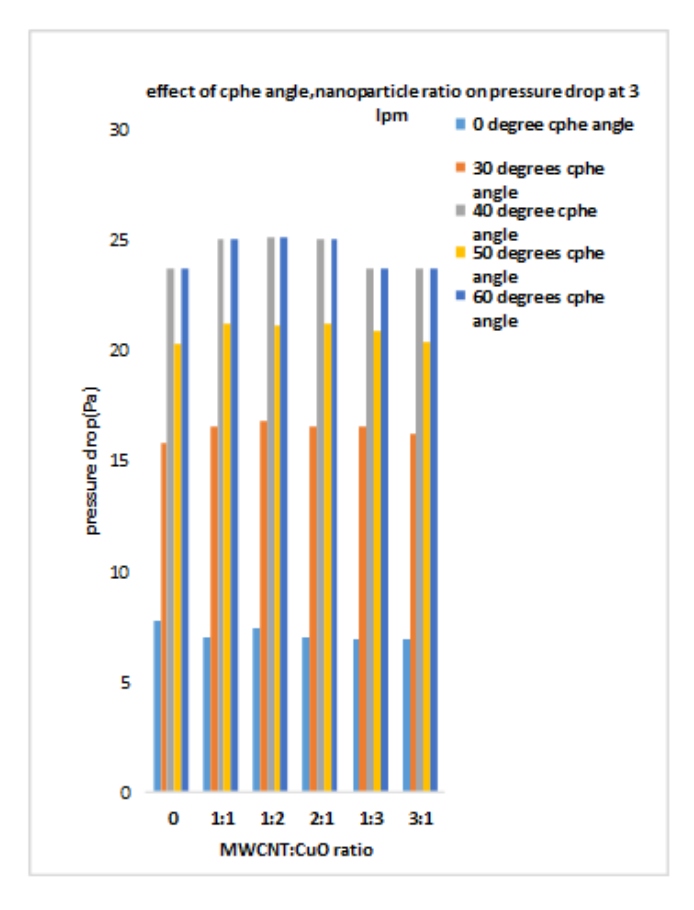


Figure 7. Effect of angle, nanoparticle ratio on pressure drop at 3 lpm

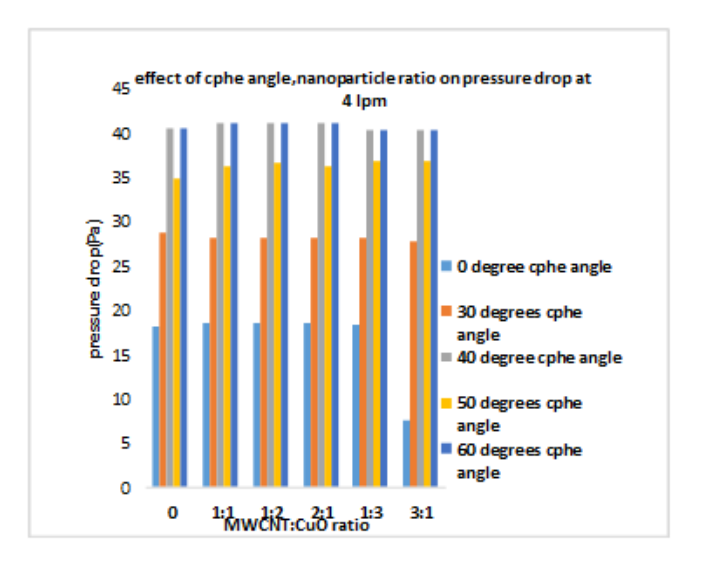


Figure 8. Effect of angle, nanoparticle ratio on pressure drop at 4 lpm

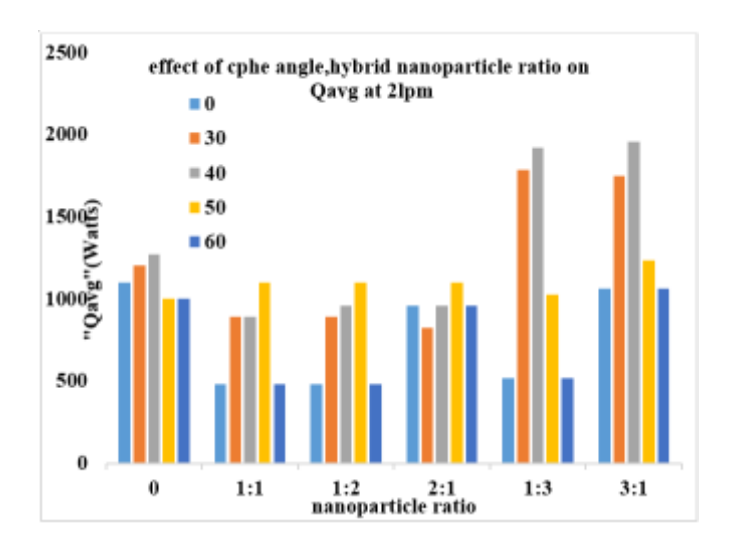


Figure 9. Effect of angle, nanoparticle ratio on Qavg at 2 lpm

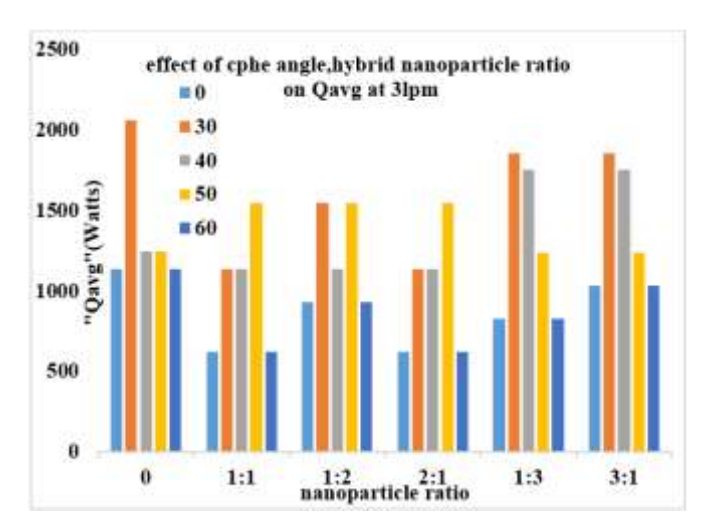


Figure 10. Effect of angle, nanoparticle ratio on Qavg at 3 lpm

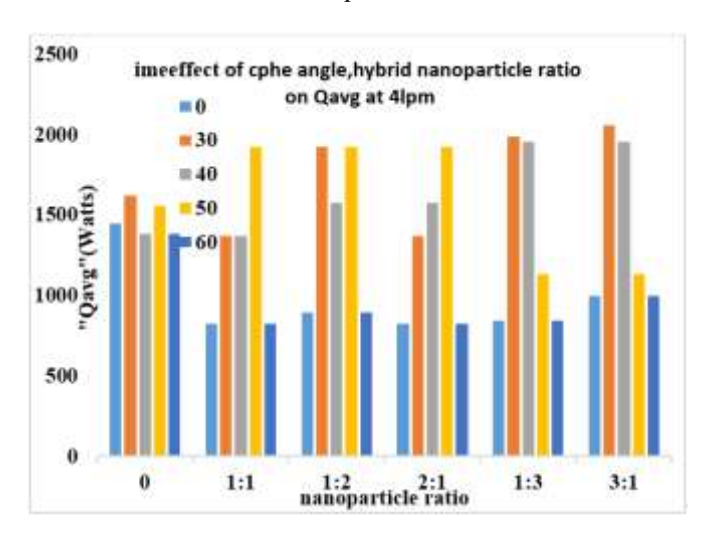


Figure 11. Effect of angle, nanoparticle ratio on Qavg at 4 lpm

The maximum $Q_{av}g$ at 2 lpm was 1953.33 W at a 40° plate angle with a 3:1 MWCNT:CuO ratio. At 3 lpm, the peak value of 2060.85 W occurred at a 30° plate angle, while at 4 lpm, the maximum was 2056.49 W at 30° with a 3:1 ratio. The increase in heat transfer rate with higher MWCNT content is attributed to the superior thermal conductivity of MWCNTs. Similarly,

increasing the volume flow rate of the hybrid nanofluid enhances the heat transfer rate due to intensified turbulence and nanoparticle Brownian motion. Maximum heat transfer was observed at a corrugation angle of 30°, where turbulence was optimized. Beyond this angle, the corrugation geometry restricted nanoparticle movement. It was also noted that while corrugations improve thermal performance, they simultaneously contribute to an increase in pressure drop.

4. CONCLUSION

It can be concluded that the maximum convective heat transfer coefficient (h) of 3021.94 W/m²K was observed at a CPHE corrugation angle of 30°, a flow rate of 4 lpm, and a 1:2 MWCNT:CuO nanoparticle ratio, corresponding to a 41% enhancement compared with the base fluid. This result is consistent with observations reported by Rafid et al. [19].

The minimum pressure drop was recorded at a 1:3 nanoparticle ratio and a flow rate of 3 lpm for the flat plate configuration, with a value of 6.90 Pa. In contrast, the maximum pressure drop occurred at a corrugation angle of 60°, a flow rate of 4 lpm, and a 3:1 MWCNT:CuO ratio, reaching 40.36 Pa. Figure 12 presents a Pareto chart generated using Minitab for pressure drop, which indicates that among the three parameters investigated, the nanoparticle ratio has an insignificant effect.

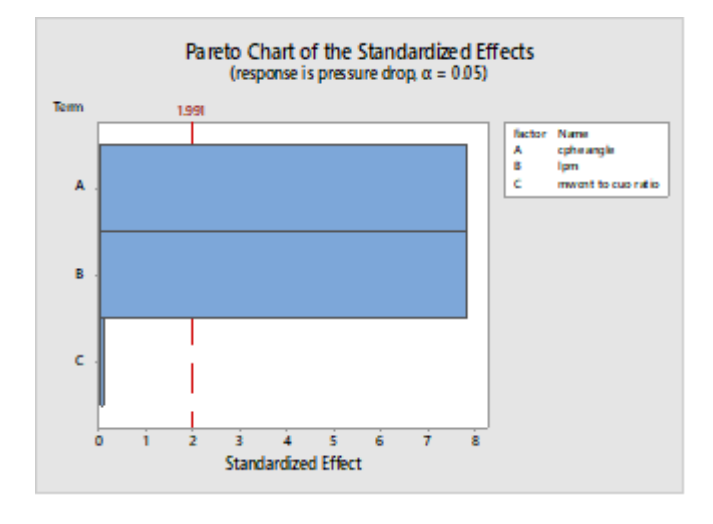


Figure 12. Pareto chart for pressure drop (Pa)

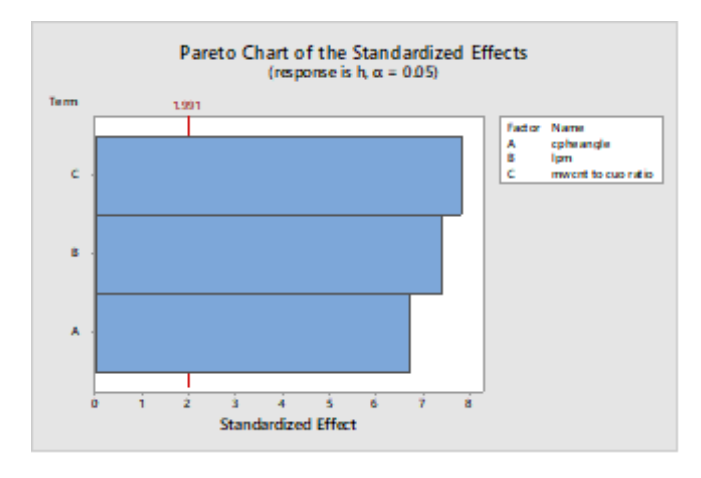


Figure 13. Pareto chart for h(W/m²K)

The results further indicate that when heat transfer

performance is the primary criterion, a corrugation angle of 30° with a 2:1 or 1:2 nanoparticle ratio is recommended. If minimization of pumping power is the main objective, a 1:3 ratio with a flat plate configuration is preferred. The effect of increasing the number of plates warrants further investigation.

Figures 13 and 14 present Pareto charts for the convective heat transfer coefficient (h) and the average heat transfer rate (Q_{av}g), showing that all three parameters are statistically significant. Design-Expert software was employed to determine the combined optimal conditions and corresponding response values. Under optimal conditions—30° corrugation angle, 2 lpm flow rate, and a 3:1 MWCNT: CuO ratio—the convective heat transfer coefficient, heat transfer rate, and pressure drop were found to be 1444.29 W/m²K, 1890.88 W, and 8.432 Pa, respectively. Figure 15 illustrates these optimal values as predicted by the Design-Expert software.

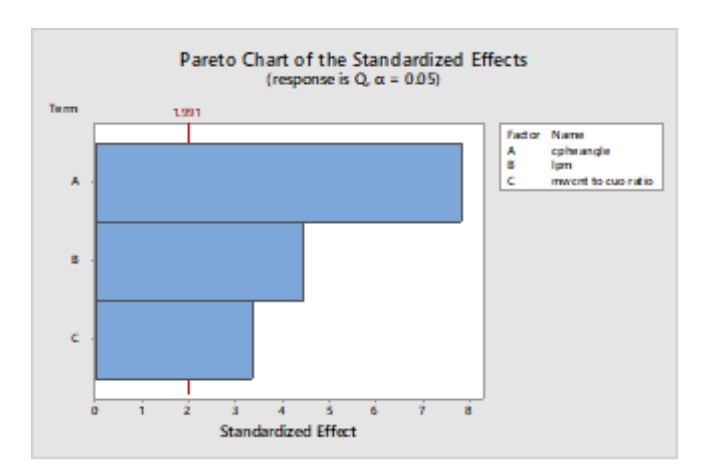


Figure 14. Pareto chart for Q(W)

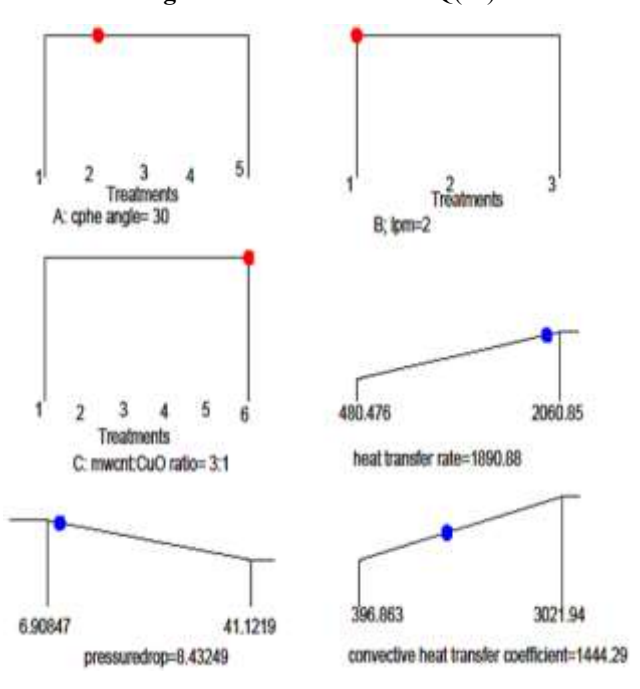


Figure 15. Optimal values derived from DesignXpert software

ACKNOWLEDGMENT

Sincere gratitude is extended by the authors to Chaitanya Bharathi Institute of Technology (CBIT) for the substantial financing and assistance.

REFERENCES

- [1] Tatsuo, N., Shinichiro, M., Shingho, A., Yuji, K. (1990). Flow observations and mass transfer characteristics in symmetrical wavy-walled channels at moderate Reynolds numbers for steady flow. International Journal of Heat and Mass Transfer, 33(5): 835-845. https://doi.org/10.1016/0017-9310(90)90067-5
- [2] Warnakulasuriya, F.S.K., Worek, W.M. (2008). Heat transfer and pressure drop properties of high viscous solutions in plate heat exchangers. International Journal of Heat and Mass Transfer, 51(1-2): 52-67. https://doi.org/10.1016/j.ijheatmasstransfer.2007.04.054
- [3] Nilpueng, K., Wongwises, S. (2015). Experimental study of single-phase heat transfer and pressure drop inside a plate heat exchanger with a rough surface. Experimental Thermal and Fluid Science, 68: 268-275. https://doi.org/10.1016/j.expthermflusci.2015.04.009
- [4] Wajs, J., Mikielewicz, D. (2016). Influence of metallic porous microlayer on pressure drop and heat transfer of stainless steel plate heat exchanger. Applied Thermal Engineering, 93: 1337-1346. https://doi.org/10.1016/j.applthermaleng.2015.08.101
- [5] Khan, T.S., Khan, M.S., Chyu, M.C., Ayub, Z.H. (2010). Experimental investigation of single phase convective heat transfer coefficient in a corrugated plate heat exchanger for multiple plate configurations. Applied Thermal Engineering, 30(8-9): 1058-1065. https://doi.org/10.1016/j.applthermaleng.2010.01.021
- [6] Godson, L., Deepak, K., Enoch, C., Jefferson, B., Raja, B. (2014). Heat transfer characteristics of silver/water nanofluids in a shell and tube heat exchanger. Archives of Civil and Mechanical Engineering, 14(3): 489-496. https://doi.org/10.1016/j.acme.2013.08.002
- [7] Wu, Z., Wang, L., Sundén, B. (2013). Pressure drop and convective heat transfer of water and nanofluids in a double-pipe helical heat exchanger. Applied Thermal Engineering, 60(1-2): 266-274. https://doi.org/10.1016/j.applthermaleng.2013.06.051
- [8] Mojarrad, M.S., Keshavarz, A., Ziabasharhagh, M., Raznahan, M.M. (2014). Experimental investigation on heat transfer enhancement of alumina/water and alumina/water—ethylene glycol nanofluids in thermally developing laminar flow. Experimental Thermal and Fluid Science, 53: 111-118. https://doi.org/10.1016/j.expthermflusci.2013.11.015
- [9] Gómez, A.O.C., Hoffmann, A.R.K., Bandarra Filho, E.P. (2015). Experimental evaluation of CNT nanofluids in single-phase flow. International Journal of Heat and Mass Transfer, 86: 277-287. https://doi.org/10.1016/j.ijheatmasstransfer.2015.02.066
- [10] Pantzali, M.N., Kanaris, A.G., Antoniadis, K.D., Mouza, A.A., Paras, S.V. (2009). Effect of nanofluids on the performance of a miniature plate heat exchanger with modulated surface. International Journal of Heat and Fluid Flow, 30(4): 691-699. https://doi.org/10.1016/j.ijheatfluidflow.2009.02.005
- [11] Javadi, F.S., Sadeghipour, S., Saidur, R., BoroumandJazi, G., Rahmati, B., Elias, M.M., Sohel, M.R. (2013). The effects of nanofluid on thermophysical properties and heat transfer characteristics of a plate heat exchanger. International Communications in Heat and Mass Transfer, 44: 58-63. https://doi.org/10.1016/j.icheatmasstransfer.2013.03.01

-7

- [12] Ray, D.R., Das, D.K., Vajjha, R.S. (2014). Experimental and numerical investigations of nanofluids performance in a compact minichannel plate heat exchanger. International Journal of Heat and Mass Transfer, 71: 732-746.
 - https://doi.org/10.1016/j.ijheatmasstransfer.2013.12.072
- [13] Sunden, B., Wu, Z., Wadsoe, L., Feng, Z. (2014). A comparative study on thermal conductivity and rheology properties of alumina and multi-walled carbon nanotube nanofluids. Frontiers in Heat and Mass Transfer, 5(1): 18. https://doi.org/10.5098/hmt.5.18
- [14] Han, Z.H., Yang, B., Kim, S.H., Zachariah, M.R. (2007). Application of hybrid sphere/carbon nanotube particles in nanofluids. Nanotechnology, 18(10): 105701. https://doi.org/10.1088/0957-4484/18/10/105701
- [15] Suresh, S., Venkitaraj, K.P., Selvakumar, P., Chandrasekar, M. (2012). Effect of Al₂O₃–Cu/water hybrid nanofluid in heat transfer. Experimental Thermal and Fluid Science, 38: 54-60. https://doi.org/10.1016/j.expthermflusci.2011.11.007
- [16] Labib, M.N., Nine, M.J., Afrianto, H., Chung, H., Jeong, H. (2013). Numerical investigation on effect of base fluids and hybrid nanofluid in forced convective heat transfer. International Journal of Thermal Sciences, 71: 163-171. https://doi.org/10.1016/j.ijthermalsci.2013.04.003
- [17] Pandey, S.D., Nema, V.K. (2012). Experimental analysis of heat transfer and friction factor of nanofluid as a coolant in a corrugated plate heat exchanger. Experimental Thermal and Fluid Science, 38: 248-256. https://doi.org/10.1016/j.expthermflusci.2011.12.013
- [18] Sarkar, J., Ghosh, P., Adil, A. (2015). A review on hybrid nanofluids: Recent research, development and applications. Renewable and Sustainable Energy Reviews, 43: 164-177. https://doi.org/10.1016/j.rser.2014.11.023
- [19] Rafid, M., Azad, A.K., Prottoy, S.M., Alam, S., et al. (2024). Augmentation of heat exchanger performance with hybrid nanofluids: Identifying research gaps and future indications-A review. International Communications in Heat and Mass Transfer, 155: 107537. https://doi.org/10.1016/j.icheatmasstransfer.2024.10753
 - https://doi.org/10.1016/j.icheatmasstransfer.2024.10753

- [20] Balashowry, K., Kumar, P.P., Prabha, K.A., Sahithi, V.V.D., Jadhav, P.K., Komble, S.P., Sable, M.J., Gawande, S.H. (2025). Nano-fluid cooled condenser in air conditioning for energy conservation. International Journal of Energy Production and Management, 10(3): 23-30. https://doi.org/10.18280/ijepm.100103
- [21] Yahya, I.Z.A., Kaedhi, H.M., Karash, E.T., Najm, W.M. (2024). Finite element analysis of the effect of carbon nanotube content on the compressive properties of zirconia nanocomposites. International Journal of Computational Methods and Experimental Measurements, 12(3): 227-235. https://doi.org/10.18280/ijcmem.120304
- [22] Nashee, S.R. (2024). Enhancement of heat transfer in nanofluid flow through elbows with varied cross-sections: A computational study. International Journal of Heat and Technology, 42(1): 311-319. https://doi.org/10.18280/ijht.420133

NOMENCLATURE

m_h	mass flow rate of hot fluid
m_c	mass flow rate of cold fluid
Q	heat transfer rate (Watts)
U	overall heat transfer rate
h	convective heat transfer coefficient (W/m ² K)
Nu	nusselt number
CP	specific heat, J. kg ⁻¹ . K ⁻¹
g	gravitational acceleration, m.s ⁻²
k	thermal conductivity, W.m ⁻¹ . K ⁻¹

Subscripts

avg average
c cold fluid
h hot water
hyb hybrid
p,np nanoparticle
w water

Greek symbols

μ dynamic viscosity, kg. m⁻¹.s⁻¹
 φ volume fraction of nanoparticle